Pure appl. geophys. 160 (2003) 467–486
0033 – 4553/03/040467 – 20



Pure and Applied Geophysics

# An Efficient Numerical Method for Computing Synthetic Seismograms for a Layered Half-space with Sources and Receivers at Close or Same Depths

HAI-MING ZHANG[1], XIAO-FEI CHEN[1] and SHYHONG CHANG[2]

*Abstract* — It is difficult to compute synthetic seismograms for a layered half-space with sources and receivers at close to or the same depths using the generalized R/T coefficient method (KENNETT, 1983; LUCO and APSEL, 1983; YAO and HARKRIDER, 1983; CHEN, 1993), because the wavenumber integration converges very slowly. A semi-analytic method for accelerating the convergence, in which part of the integration is implemented analytically, was adopted by some authors (APSEL and LUCO, 1983; HISADA, 1994, 1995). In this study, based on the principle of the Repeated Averaging Method (DAHLQUIST and BJÖRCK, 1974; CHANG, 1988), we propose an alternative, efficient, numerical method, the *peak-trough averaging method* (PTAM), to overcome the difficulty mentioned above. Compared with the semi-analytic method, PTAM is not only much simpler mathematically and easier to implement in practice, but also more efficient. Using numerical examples, we illustrate the validity, accuracy and efficiency of the new method.

**Key words:** Numerical integration method, layered half-space, synthetic seismograms, the peak-trough averaging method.

## *Introduction*

Computing synthetic seismograms in a layered half-space is an important tool for investigating the interior structure of the earth as well as the dynamic process of seismic sources from well-recorded seismic data. Since the 1970s, many endeavors have been made regarding the calculation of Green's functions in seismological studies (FUCHS and MÜLLER, 1971; HELMBERGER, 1974; BOUCHON and AKI, 1977; BOUCHON, 1979; KENNETT and KERRY, 1979; WANG and HERRMANN, 1980; LUCO and APSEL; 1983; APSEL and LUCO, 1983; KENNETT, 1983; YAO and HARKRIDER, 1983; DRAVINSKI and MOSSESSIAN, 1988; CHEN, 1993, 1999; HISADA, 1994, 1995). According to the generalized R/T coefficient method (KENNETT, 1983; CHEN, 1999), the Green's function due to an arbitrary point seismic source buried in a layered

[1] Department of Geophysics, Peking University, Beijing 100871, China. E-mail: xfchen@pku.edu.cn
[2] Price Bargain Inc., Los Angeles, CA 90072, U.S.A.

half-space can be expressed as a summation of the products of radiation patterns and the following type of oscillatory integrals,

$$I_n(\omega) = \int_0^{+\infty} F(\omega, k) \cdot J_n(kr)\, dk \ , \tag{1}$$

where $r$ is the epicentral distance, $k$ is the horizontal wavenumber and $\omega$ is the circular frequency. $F(\omega, k)$ is the kernel function which includes a decaying factor $\exp(-\zeta^{(j)}|z^{(j)} - z^{(j-1)}|)$, $\exp(-\zeta^{(j)}|z - z^{(j)}|)$ or $\exp(-\zeta^{(j)}|z - z_s|)$, in which $\zeta^{(j)} = \sqrt{k^2 - (\omega/c^{(j)})^2}$ ($c^{(j)}$ is the wave velocity in the $j$-th layer) (see, CHEN, 1993). The depths of the receiver, the $j$-th interface and the source are represented by $z$, $z^{(j)}$, and $z_s$, respectively, and $J_n(kr)$ is the Bessel function of order $n$. The speed of convergence of the integrand in equation (1) is determined by both the kernel function and the Bessel function. When the sources and receivers are at close to or the same depths, both the kernel function and the Bessel function converge very slowly with $k$ making the integral difficult to compute numerically. To explore the numerical convergence of integral (1), we introduce the following definite integral,

$$P_n(\omega, k) = \int_0^{k} F(\omega, \tilde{k}) \cdot J_n(\tilde{k}r)\, d\tilde{k} \ , \tag{1a}$$

where

$$I_n(\omega) = \lim_{k \to +\infty} \{P_n(\omega, k)\} \ .$$

We call $P_n(\omega, k)$ the partial integral of $I_n(\omega)$. Figures 1(a)–(c) show the kernel function $F(\omega, k)$, the integrand $F(\omega, k) \cdot J_n(kr)$ $(n = 2)$, and the partial integral $P_n(\omega, k)$ respectively, versus wavenumber $k$ for a particular layered media (Crust Model 2 in Table 3) at $f = 1.0$ Hz. Since the imaginary parts of the integrand and the partial integral converge more quickly than those of real parts (CHANG, 1988; HISADA, 1994), only the real parts are shown. We can see that both the integrand and partial integral converge very slowly. It is expected that the partial integral will converge at very large $k$, however, the corresponding computation is too expensive to implement. One remedy for this kind of problem is the semi-analytical method (abbreviated to SAM, see APSEL and LUCO, 1983; HISADA, 1994, 1995), in which the integral is broken into two parts; one of them is carried out analytically (we call them *numerical integral* and *analytic integral*, respectively, for the convenience in description). The prime merit of the semi-analytic method is that the integration interval of the numerical integral is greatly reduced. However, on the one hand, to what extent the integration interval is reduced depends heavily on the choice of the analytic integral. Usually such a choice is rather complicated mathematically (HISADA, 1994, 1995). On the other hand, since the result of the analytic integral is an

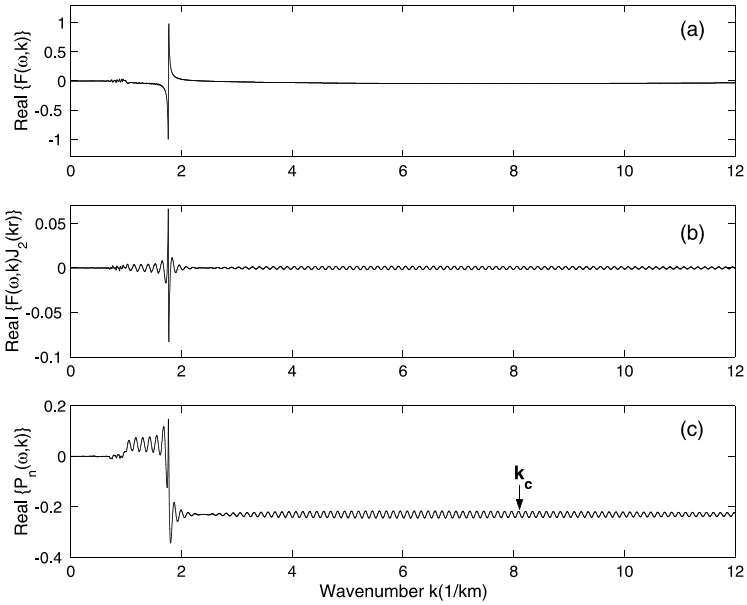


Figure 1
(a)–(c) Real parts of the kernel function $F(\omega, k)$, the integrand $F(\omega, k) \cdot J_n(kr)$ (for $n = 2$), and the partial integral $P_n(\omega, k)$ versus wavenumber $k$ at a given frequency ($f = 1.0$ Hz). $k_c$ in (c) is the critical wavenumber, beyond which the partial integral $P_n(\omega, k)$ becomes an oscillatory curve with a monotonically and smoothly decaying envelope. Crust Model 2 (see Table 3) is used. Here the epicentral distance is $r = 50$ km, the focal depth is $z_s = 0.3$ km, and the receiver depth is $z_0 = 0.0$ km. Notice that all traces here are normalized by the maximum amplitude of the top curve.

exact one, the integration step in the numerical integral, which is implemented numerically, must be very small to reduce the discrepancy in preciseness of the two integrals. Consequently, although the integration interval in the numerical integral is greatly reduced, considerable numerical computation is still involved.

In this study we propose an alternative method, the *Peak-Trough Averaging Method* (PTAM), based on the principle of the Repeated Averaging Method (DAHLQUIST and BJÖRCK, 1974; CHANG, 1988). The Repeated Averaging Method (RAM) is an efficient approach for evaluating the convergent values of slowly convergent alternating sequences (DAHLQUIST and BJÖRCK, 1974). As shown in Figure 1(c), beyond a critical wavenumber $k_c$, the partial integral $P_n(\omega, k)$ becomes an oscillatory curve with a monotonically and smoothly decaying envelope, indicating that the process is slowly approaching its convergent point, $I_n(\omega)$. The distribution of the peaks and troughs of this slowly convergent partial integral behaves like a monotonically decaying alternating sequence, thus it can be efficiently evaluated by applying RAM. Such an integral evaluation method is named the Peak-Trough Averaging Method. Compared with the semi-analytic approach, PTAM is much simpler mathematically and easier to implement in practice. By using a numerical

test, we will demonstrate that the precision of PTAM is slightly higher than that of SAM with the same integration step and truncated upper limit, and PTAM is more efficient than SAM. In what follows we shall first briefly introduce the repeated averaging method, then describe its application to the evaluation of slowly convergent integrals of the kind of integral (1), i.e., introduce the peak-trough averaging method. Finally we will demonstrate the accuracy, efficiency and applicability of the new method by numerical examples.

## *Fundamentals of the Repeated Averaging Method*

To explore our new efficient integration method, we shall first briefly introduce the *Repeated Averaging Method* (RAM) by considering the evaluation of the following slowly convergent alternating series (DAHLQUIST and BJÖRCK, 1974),

$$1-\frac{1}{3}+\frac{1}{5}-\frac{1}{7}+\frac{1}{9}-\frac{1}{11}+\cdots+\frac{(-1)^n}{2n+1}+\cdots \quad . \tag{2}$$

This series very slowly converges to its sum, $\pi/4$. We can define a corresponding sequence $\{M_0(n); n=1,2,\ldots\}$ as follows:

$$M_0(n)=\sum_{i=1}^{n}\frac{(-1)^{i-1}}{2i-1} \quad . \tag{2a}$$

Obviously, the limit of this sequence equals the sum of the original series (2), namely,

$$\lim_{n\to+\infty}\{M_0(n)\}=\frac{\pi}{4} \quad .$$

Hence, in what follows we shall discuss how to efficiently evaluate the limit of the sequence $\{M_0(n); n=1,2,\ldots\}$ rather than the sum of the original series (2). As shown in Figure 2(a), the partial sum sequence $M_0(n)$ converges to $\pi/4$ very slowly. $M_0(n)$ alternates around its limit $\pi/4$ with a monotonically and smoothly decaying envelope. To describe the convergence speed of the sequence $\{M_0(n)\}$, we define a relative error sequence $E_0(n)$ of $M_0(n)$ to its limit as follows,

$$E_0(n)=\frac{|M_0(n)-M_0(+\infty)|}{|M_0(+\infty)|} \quad . \tag{3}$$

Obviously, $E_0(n)\to 0$ as $n\to+\infty$. Figure 2(b) displays the distribution of relative error sequence $E_0(n)$ that indicates the convergence speed of $M_0(n)$. It can be seen that the convergence speed of $M_0(n)$ is very slow. Accordingly, the usual direct evaluation of this kind of slowly convergent alternating sequence is very time-consuming and thus is less efficient. Fortunately, a method called the Repeated Averaging Method (RAM) described by DAHLQUIST and BJÖRCK (1974) can

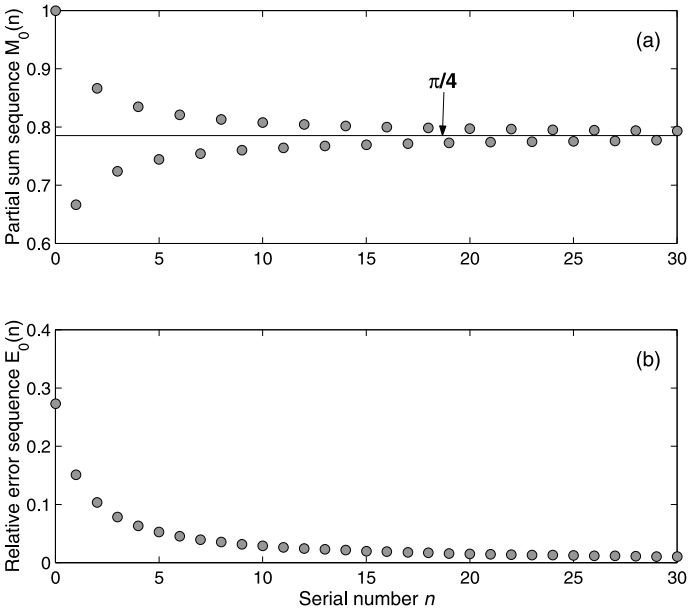


Figure 2
(a) The partial sum sequence $M_0(n)$ (see equation (2a) in the text) alternates around its limit point $\pi/4$ with a monotonously and smoothly decaying envelope. (b) The distribution of the relative error sequence $E_0(n)$, which indicates the speed of convergence of $M_0(n)$.

dramatically improve the evaluation efficiency of this kind of slowly convergent alternating sequence.

To explain the basic idea of RAM clearly, we first define the *i*-th order *reduced sequence* $M_i(n)$ and the corresponding *relative error sequence* $E_i(n)$ as follows,

$$M_i(n) = \frac{1}{2}[M_{i-1}(n+1) + M_{i-1}(n)] \quad (i = 1, 2, 3 \ldots) \tag{4a}$$

$$E_i(n) = \frac{|M_i(n) - M_i(+\infty)|}{|M_i(+\infty)|} \quad (i = 1, 2, 3 \ldots) \ , \tag{4b}$$

where $M_0(n)$ is defined in equation (2a). Since the limit of the sequence $M_0(n)$ does exist, we can show that all the reduced sequences $M_i(n)$ $(i = 1, 2, 3 \ldots)$ converge to the same limit as that of $M_0(n)$ as follows.
For $i = 1$,

$$\begin{aligned} \lim_{n \to +\infty} M_1(n) &= \frac{1}{2}\left[\lim_{n \to +\infty} M_0(n+1) + \lim_{n \to +\infty} M_0(n)\right] \\ &= \frac{1}{2}[M_0(+\infty) + M_0(+\infty)] = M_0(+\infty) \ . \end{aligned} \tag{5a}$$

Likewise, using the iterative relation (4a) one can easily show the results for $i > 1$ below,

$$M_i(+\infty) = M_{i-1}(+\infty) = \cdots = M_1(+\infty) = M_0(+\infty) \ . \tag{5b}$$

Another notable property of the reduced sequence $M_i(n)(i = 1, 2, 3 \ldots)$ is its speed of convergence. As shown in Figure 3, the higher order reduced sequences converge to the limit value more rapidly than the lower order ones, and the higher the order is, the more rapidly the reduced sequence $M_i(n)$ converges to the limit value than the original sequence $M_0(n)$. Accordingly, the relative error function $E_i(n)$ more rapidly goes to zero. For instance, $E_0(n) < 10^{-6}$ for $n > 3 \times 10^5$, i.e., $\{|M_0(n) - M_0(\infty)|/|M_0(\infty)|\} < 10^{-6}$ for $n > 3 \times 10^5$. This means that with an accuracy of $10^{-6}$, the usual direct evaluation of infinite series (2) needs at least $3 \times 10^5$ terms. However, as seen from Figure 3, the sixth-order reduced sequence $\{M_6(n)\}$ converges so fast that $n$ is only required to be greater than 5 for the same accuracy. Thus $\{|M_6(n) - M_6(\infty)|/|M_6(\infty)|\} < 10^{-6}$ for $n > 5$, which is five orders of magnitude faster than the usual direct evaluation of the sum of infinite series (2) or the limit of sequence $\{M_0(n); n = 1, 2, \ldots\}$. On the other hand, all the higher order reduced sequences converge to the *same* limit as demonstrated in equation (5). Therefore we can evaluate the limit of higher order reduced sequence $\{M_i(n); n = 1, 2, \ldots\}$, rather than directly evaluate the limit of the original sequence $\{M_0(n); n = 1, 2, \ldots\}$, so that the computation efficiency will be dramatically

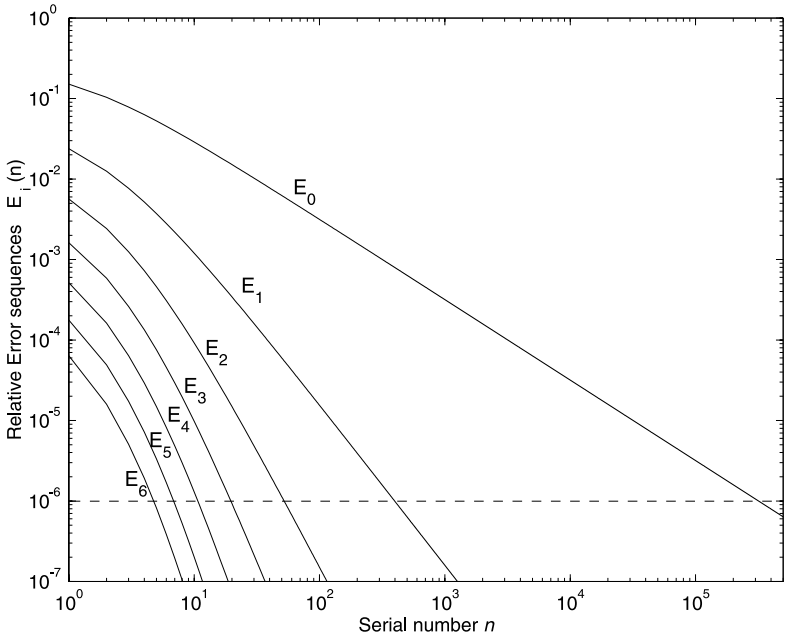


Figure 3
Distribution of relative error sequences $E_i(n)$ of different orders. The higher order reduced sequences converge to the limit value more rapidly than the lower order ones.

improved as shown above. Such an evaluation is not only mathematically efficient, but also easy to implement for computer calculation. Table 1 illustrates the arithmetic evaluation process, in which each term of the higher order reduced sequence is simply generated by the arithmetic mean of the corresponding pair of neighbor terms of the previous lower order reduced sequence as indicated by the short lines. It should be recognized that to generate the $n$-th term of the $i$-th reduced sequence $M_i(n)$, the first $(n+i)$ terms of the original infinite series are needed, according to the definition of $M_i(n)$ given in equation (4a). In summary, RAM is not only very efficient and accurate but also a very simple algorithm to evaluate an alternating series or the limit of an alternating sequence (DAHLQUIST and BJÖRCK, 1974).

## *The Peak-trough Averaging Method*

We now consider how to efficiently evaluate the integral (1) by applying RAM. As shown in Figure 1(c), beyond a critical $k_c$, the partial integral $P_n(\omega, k)$ becomes an oscillatory function with a monotonically and smoothly decaying envelope, indicating the process of slowly approaching its limit, $I_n(\omega)$. The behavior of the peaks and troughs of this slowly convergent function acts like an alternating sequence, which suggests adopting RAM to efficiently evaluate the slowly convergent integral (1) by the following procedures.

First, determine the critical $k_c$ beyond which the partial integral $P_n(\omega, k)$ becomes an oscillatory function with a monotonically and smoothly decaying envelope. The critical wavenumber $k_c$ can be determined by an empirical formula

$$k_c = 1.5 \times |\omega| / v_{\min} \ , \tag{6}$$

where $v_{\min}$ is the minimum velocity of the structure model, $\omega$ is the circular frequency. When the discrete wavenumber integration method (see e.g., BOUCHON and AKI, 1977) is used, an imaginary frequency is introduced to depress the influence

Table 1

*Arithmetic evaluation process of the Repeated Averaging Method. The bits which are different in higher order reduced sequences $M_i$ $(i = 1, 2, \ldots, 6)$ are underlined*

| $n$ | $M_0$ | $M_1$ | $M_2$ | $M_3$ | $M_4$ | $M_5$ | $M_6$ |
|---|---|---|---|---|---|---|---|
| 5 | 0.744012 | 0.782474 | 0.785038 | 0.785340 | 0.785387 | 0.785396 | 0.785398 |
| 6 | 0.820935 | 0.787602 | 0.785641 | 0.785434 | 0.785405 | 0.785400 | |
| 7 | 0.754268 | 0.783680 | 0.785228 | 0.785376 | 0.785395 | | |
| 8 | 0.813092 | 0.786776 | 0.785523 | 0.785414 | | | |
| 9 | 0.760460 | 0.784270 | 0.785305 | | | | |
| 10 | 0.808079 | 0.786340 | | | | | |
| 11 | 0.764601 | | | | | | |

of fictitious sources and structures. In such a case, $\omega = \omega_R + i\omega_I$, where $\omega_R$ and $\omega_I$ is the real and imaginary circular frequency, respectively. As mentioned earlier, the kernel function $F(\omega, k)$ in the $j$-th layer includes a decaying factor $\exp(-\zeta^{(j)}|z - z_s|)$, with $\zeta^{(j)} = \sqrt{k^2 - (\omega/c^{(j)})^2}$ ($c^{(j)}$ is the wave velocity in the $j$-th layer). Obviously, $\exp(-\zeta^{(j)}|z - z_s|)$ behaves as an oscillatory function when $k < |\omega|/c^{(j)}$; however, it becomes a decaying factor when $k > |\omega|/c^{(j)}$. Consequently, $|\omega|/v_{\min}$ is a critical point, beyond which the partial integral $P_n(\omega, k)$ decays with the increase of upper limit $k$ (see, Figure 1(c)). Usually in practice, an empirical coefficient, such as 1.5 in equation (6), is added to ensure the decaying property of $P_n(\omega, k)$.

Second, determine the raw peaks and troughs of the curve of $P_n(\omega, k)$ versus $k$ in the range of $k$ greater than $k_c$ by the following simple screening process as the integral evaluation continues. As $k$ ($k > k_c$) increases with a fixed step-size $\Delta k$ (in discrete wavenumber integration method, $\Delta k = 2\pi/L$, see, BOUCHON and AKI, 1977), we record every three successive integral sampling points $k_i$ and the corresponding values of the partial integral $S_i$ ($= P_n(\omega, k_i)$), i.e., $(k_i, S_i)(i = 1, 2, 3)$. If $S_2$ is larger or smaller than both $S_1$ and $S_3$, then $(k_2, S_2)$ is a rough location of a peak or trough. If not, there is no peak or trough found in this interval. Regardless of the case, move forward one point and form a new three successive integral sampling points and the partial integral values $(k_i', S_i')(i = 1, 2, 3)$, then repeat the above screening procedure until enough peaks and troughs are found.

Finally, regard the sequential peaks and troughs as an alternating sequence, and apply RAM to evaluate the limit value that equals $I_n(\omega)$. As shown in Figure 1(c), the sequential distribution of those peaks and troughs behaves like an alternating sequence (hereafter we call it a *peak-trough sequence*) whose limit is believed to be the same as the convergent value of the partial integral $P_n(\omega, k)$, i.e., $I_n(\omega)$. This allows us to adopt the efficient algorithm, RAM, to evaluate the integral $I_n(\omega)$ through evaluating the limit value of the *peak-trough sequence*. Therefore, we designate this efficient integration method as the *Peak-Trough Averaging Method* (PTAM).

It is noted that the accuracy of this approach heavily depends on the accuracy of the values of those peaks and troughs. However, the raw values of peaks and troughs obtained by the above screening process are not accurate enough, and must be further refined. This can be achieved by a simple quadratic interpolation technique. We construct the following quadratic interpolation polynomial

$$S(k) = a_1 \left( \frac{k - k_1}{k_3 - k_1} \right)^2 + a_2 \left( \frac{k - k_1}{k_3 - k_1} \right) + a_3 \ , \tag{7}$$

where $a_1 = 2S_3 - 4S_2 + 2S_1$, $a_2 = 4S_2 - S_3 - 3S_1$, $a_3 = S_1$, and $S_i = S(k_i)$ $(i = 1, 2, 3)$, and the coordinates of the refined peak (when $a_1 < 0$) or trough (when $a_1 > 0$) can be easily found as

$$\left(k_1 - \frac{a_2}{2a_1}(k_3 - k_1),\ \ S_1 - \frac{a_2^2}{4a_1}\right) .$$

Applying the above process to all raw peaks and troughs, we can obtain a set of refined peaks and troughs. Figure 4 shows an example of refining the location and peak value from a raw location and peak value $(k_2, S_2)$. The dashed line is a simple sine function; the analytic form of which is assumed to be unknown in a practical computation, and the cross and asterisk are the accurate peak and refined peak obtained by using the above technique, respectively. It can be seen that the refined peak $(k^*, S^*)$ is decidedly more accurate than the raw one; actually, the absolute error of $S^*$ to the accurate value is less than $10^{-5}$, whereas the error of the raw one is about $2.5 \times 10^{-3}$. Having these accurate peaks and troughs, we can directly apply the RAM to evaluate the limit value of the related peak-trough sequence, and thus obtain the integration value of equation (1).

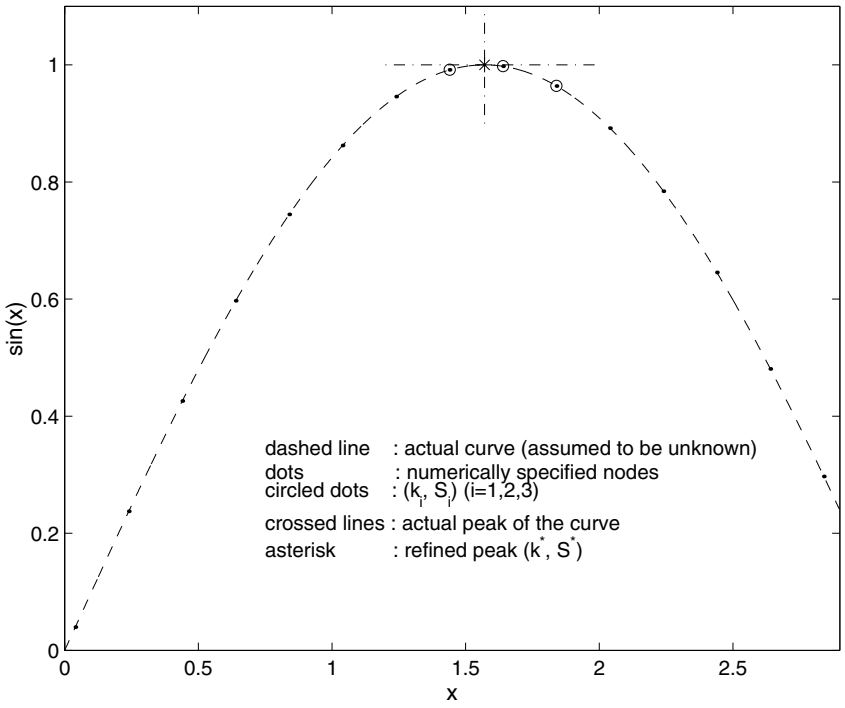


Figure 4

An example of refining the location and peak value from a raw peak $(k_2, S_2)$. Here the dashed line is $\sin(x)$, the analytic form of which is assumed to be unknown in practical numerical computation. The dots represent the numerically specified nodes, the circled dots represent the three successive points $(k_i, S_i)(i = 1, 2, 3)$ to be interpolated, and the asterisk and cross represent the refined peak $(k^*, S^*)$ and the accurate value, respectively. The absolute error of $S^*$ to the accurate value is less than $10^{-5}$, while the error of the raw one is about $2.5 \times 10^{-3}$.

## *Validation and Application of PTAM*

### *Validity of PTAM*

We shall consider two well-known examples to test the validity of PTAM. The first example considered is the calculation of synthetic scalar wave field in an infinite homogeneous and isotropic media. This problem has the following analytic solution (see, e.g., AKI and RICHARDS, 1980):

$$\phi(x,y,z,t) = \frac{f(t-R/c)}{2\pi R} \quad , \tag{8}$$

where $R = \sqrt{z^2 + r^2}$, and $c$ is the velocity of the wave. In the frequency domain, the above solution has the form of

$$\bar{\phi}(x,y,z,\omega) = G(\mathbf{x},\omega)F(\omega) \quad ,$$

where $F(\omega)$ is the spectrum of the source-time function $f(t)$ and

$$G(\mathbf{x},\omega) = \frac{\exp(-i\omega R/c)}{R} \quad . \tag{9}$$

Notice that $G(\mathbf{x},\omega)$ can be represented by the superposition of a set of cylindrical waves via the following Sommerfeld integral (see, e.g., AKI and RICHARDS, 1980):

$$G(\mathbf{x},\omega) = \int_0^{+\infty} \frac{\exp[-\gamma(k)|z|]}{\gamma(k)} J_0(kr)k\,dk \quad , \tag{10}$$

where $\gamma(k) = \sqrt{k^2 - (\omega/c)^2}$ with $\mathrm{Re}\{\gamma(k)\} \geq 0$. The reason for taking this problem as an example is not only its analytic solution, but also its similarity to the formulation of the general problem of seismic wave propagation in layered media (see, e.g., KENNETT, 1983; CHEN, 1999). For the case of $|z| \sim 0$, integral (10) becomes a slowly convergent integral, and the usual direct integration method will be less efficient. We shall apply PTAM algorithm to evaluate this integral, and compare it with the semi-analytic method (SAM) and direct integration method.

Due to the pole on the integration path, the Sommerfeld integral in equation (10) is an improper integral. However, it can be converted to a proper integral as follows:

$$\int_0^{+\infty} \frac{\exp[-\gamma(k)|z|]}{\gamma(k)} J_0(kr)k\,dk = I_1 + I_2 \quad , \tag{11}$$

where,

$$I_1 = -2i \int_0^{\sqrt{\frac{\omega}{c}}} \frac{\exp[-i\cdot q\sqrt{2\omega/c - q^2}|z|]}{\sqrt{2\omega/c - q^2}} \left(\frac{\omega}{c} - q^2\right) J_0\left[\left(\frac{\omega}{c} - q^2\right)r\right] dq \quad , \tag{11a}$$

and

$$I_2 = 2\int_0^{+\infty} \frac{\exp[-q\sqrt{2\omega/c+q^2}|z|]}{\sqrt{2\omega/c+q^2}}\left(\frac{\omega}{c}+q^2\right)J_0\left[\left(\frac{\omega}{c}+q^2\right)r\right]dq \ . \tag{11b}$$

Notice that there are no poles on the integration paths of $I_1$ and $I_2$, and the integrand in $I_2$ is a purely real function. Since the integration interval of $I_1$ is limited, it can be calculated by using a standard numerical integration technique. Thus we will focus on the calculation of $I_2$.

In SAM, the integral in equation (10) can be rewritten as

$$\begin{aligned}\int_0^{+\infty} \frac{\exp[-\gamma(k)|z|]}{\gamma(k)}J_0(kr)k\,dk = &\int_0^{+\infty}\left\{\frac{\exp[-\gamma(k)|z|]}{\gamma(k)}k-\exp[-k|z|]\right\}J_0(kr)dk \\ &+\int_0^{+\infty}\exp[-k|z|]J_0(kr)\,dk \ ,\end{aligned} \tag{12}$$

where

$$\int_0^{+\infty}\exp[-k|z|]J_0(kr)\,dk = 1/R = 1/\sqrt{z^2+r^2} \ . \tag{12a}$$

(GRADSHTEYN and RYZHIK, 1980). Equation (12) can also be converted to a proper integral similar to equation (11).

The integrand in $I_2$ versus variable $q$ and $I_2$ versus the truncated upper limit $q_{\max}$ for $z = 0.01$ km and $f = 3.0$ Hz are shown (solid lines) in Figures 5(a) and (b), respectively. For comparison, the corresponding integrand in the numerical integral of SAM is shown (dot-dash line) in Figure 5(a). We can see that the integrand of SAM converges more rapidly than that of PTAM. In Figure 5(b), the calculated integral value of $I_2$ using PTAM is indicated as a straight line, and the peaks and troughs are represented as asterisks. The accurate value of $I_1 + I_2$ and those of PTAM and SAM and the corresponding relative errors are listed in Table 2, in which the integration step and truncated upper limit of SAM are the same as those of PTAM. As we can see, both methods have a high precision.

To demonstrate the result in time domain, we choose the Ricker wavelet (RICKER, 1977) as the source time function:

$$f(t) = \frac{\sqrt{\pi}}{2}\left(\frac{u^2}{4}-\frac{1}{2}\right)\exp\left(-\frac{u^2}{4}\right) \tag{13}$$

with $u = 2\sqrt{6}(t-t_0)/t_b$, where $t_0$ and $t_b$ are the shift time and the width between the two peaks, respectively. The comparison of PTAM, SAM and the accurate value and

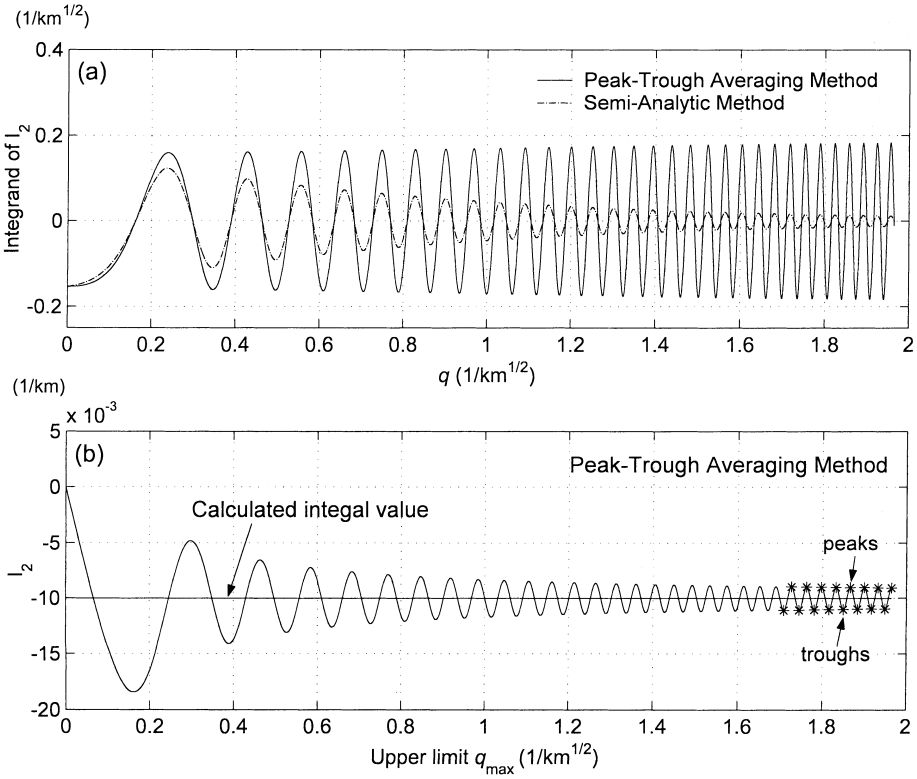


Figure 5
(a) The integrand in $I_2$ versus variable $q$ $(1/\mathrm{km}^{1/2})$ for $z = 0.01$ km and $f = 3.0$ Hz is shown by a solid line. The corresponding integrand in the numerical integral of the semi-analytic method is also shown by a dot-dash line. (b) $I_2$ versus the truncated upper limit $q_{\max}$. The calculated integral value of $I_2$ using PTAM is indicated as a straight line, and the peaks and troughs are represented as asterisks.

Table 2

*Comparison of results and the relative errors by using PTAM and SAM*

| Accurate value (1/km) | | Real part | Imaginary part |
|---|---|---|---|
| | | $-9.999088 \times 10^{-3}$ | $1.732102 \times 10^{-2}$ |
| PTAM | Value (1/km) | $-1.001710 \times 10^{-2}$ | $1.732054 \times 10^{-2}$ |
| | Relative Error | 0.180096% | 0.028169% |
| SAM | Value (1/km) | $-9.954172 \times 10^{-3}$ | $1.732054 \times 10^{-2}$ |
| | Relative Error | 0.449199% | 0.028169% |

the relative errors of PTAM and SAM are shown in Figures 6(a) and (b), respectively. Here $t_0 = 5.0$ s, $t_b = 3.0$ s. The relative error is defined as the ratio of the absolute error and the maximum amplitude of $\phi(x, y, z, t)$. The maximum relative errors of PTAM and SAM are both less than 0.1%, implying that both methods are

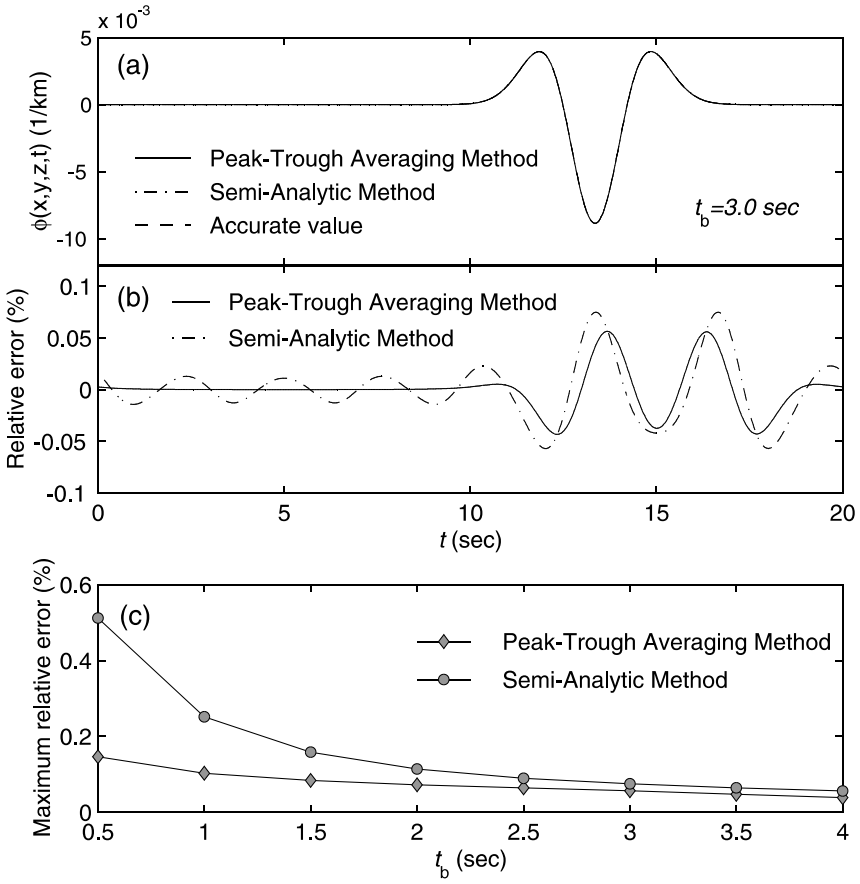


Figure 6
(a) Comparison of $\phi(x, y, z, t)$ by using PTAM, SAM and the accurate solution ($t_0 = 5.0$ s, $t_b = 3.0$ s). (b) Relative errors of PTAM and SAM. (c) Comparison of the maximum relative errors of PTAM (line with diamonds) and SAM (line with circles) versus $t_b$.

accurate. Figure 6(c) illustrates the comparison of the maximum relative errors of PTAM and SAM versus $t_b$. Note that the integration steps and the truncated upper limits for both methods are the same. As shown, the larger $t_b$ is, the smaller the maximum relative error is, and for the same $t_b$, the precision of PTAM is slightly higher than that of SAM.

Having proved the accuracy, we proceed to demonstrate the efficiency of PTAM. Figure 7 shows the comparison of the computation time of PTAM, SAM and direct integration method for various parameter $z$, which is a crucial parameter for the convergence of integral (10). For each $z$, we use PTAM with six peaks and six troughs, the computation time is shown as a line with diamonds. For the same precision as PTAM at each $z$, SAM and the direct integration is performed and the

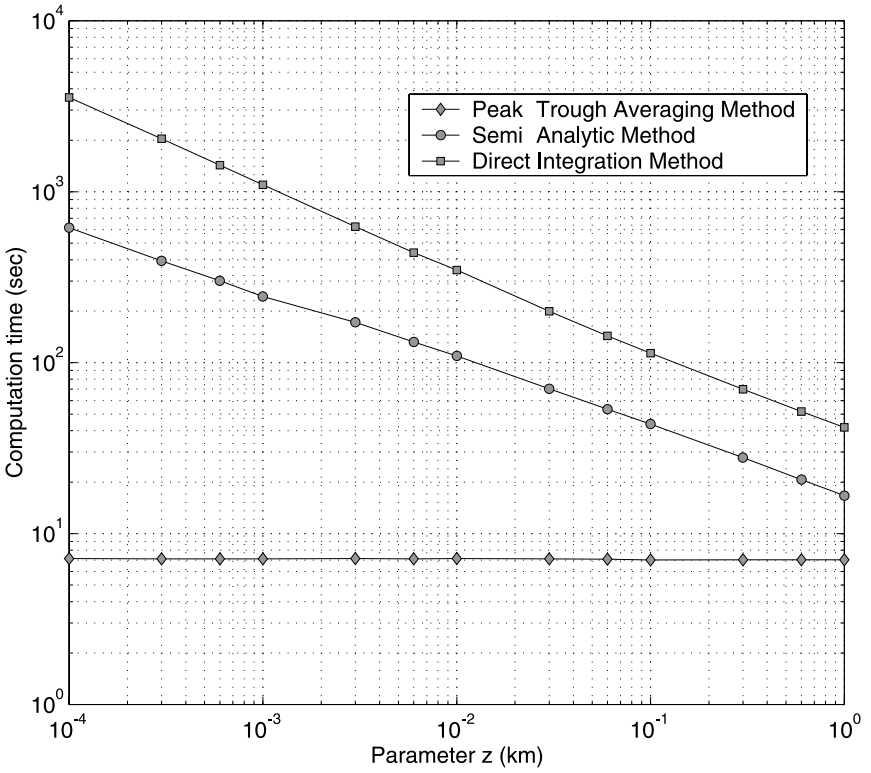


Figure 7
Comparison of the computation time of PTAM (line with diamonds), SAM (line with circles) and the direct integration method (line with squares) for different parameter $z$.

corresponding computation time is plotted as lines with circles and squares, respectively. It is obvious that with the decrease of $z$, the computation time of SAM and the direct integration method increase dramatically, whereas the computation time of PTAM remains unchanged. Although the integration interval is greatly reduced and considerable computation time is saved compared with the direct integration method, SAM proves to be much less efficient than PTAM when $z$ tends to zero.

The second example for the validity of PTAM is the classical Lamb's problem (LAMB, 1904). The original Lamb's problem involved the computation of the response at surface of a semi-infinite isotropic elastic solid due to a vertical point force applied at the surface. A closed form solution of the integral solution was given by LAMB (1904). We compute the response using the generalized R/T coefficient method (KENNETT, 1983; CHEN, 1999) with PTAM and Lamb's formulae, respectively. A Poisson solid with a $P$-wave velocity of 5 km/s is used. The epicentral distance is 67 km, and the source time function is $p/(t^2 + p^2)$ with $p = 0.15$ s.

Figure 8 presents the comparison of the two results. As shown, the waveforms with the two completely different methods are in very good agreement, which again indicates that the PTAM is accurate.

*Application to Calculation of Synthetic Seismograms*

Having illustrated the validity and efficiency of PTAM using numerical examples, we now apply it to the calculation of synthetic seismograms.

We first consider a two-layer crust model (Crust Model 1, see Table 3). The source is a strike-slip double-couple point source at the surface, and the receivers are also at the surface and aligned from 30 km to 200 km set apart with a step of 5 km and an azimuth of 30°. The source time function here is a smoothed ramp function (BOUCHON, 1982) with a rise time 0.2 s. The synthetic three-component displacement seismograms are shown in Figure 9, where reduced time $t - R/\alpha_1$ is used ($R$ is the epicentral distance and $\alpha_1$ is the $P$-wave velocity in the top layer). The main theoretical arrival time curves are also plotted. The waveforms of vertical and radial

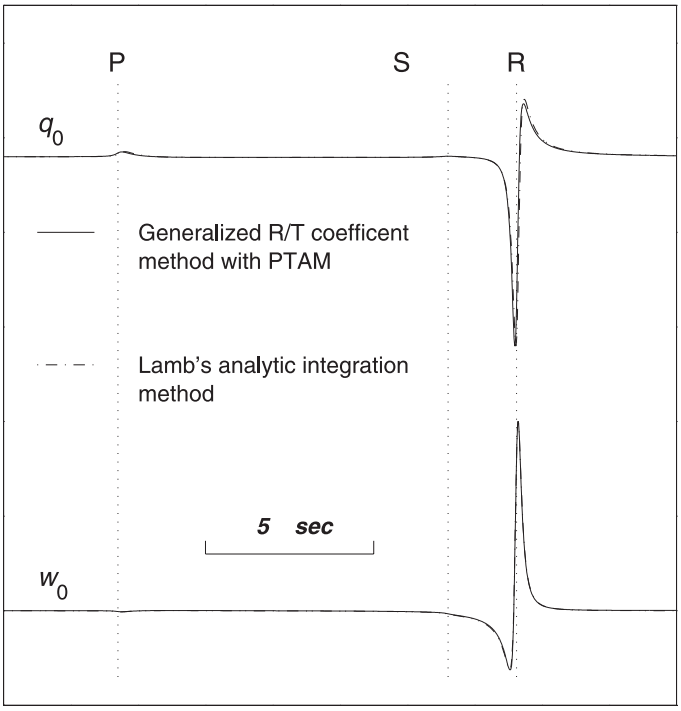


Figure 8
Comparison of the results of Lamb's problem by using the generalized R/T coefficient method with PTAM and Lamb's analytic integration method.

Table 3

*Layered crust models*

| Layer Thickness (km) | *P*-wave Velocity (km/s) | *S*-wave Velocity (km/s) | Density (g/cm$^3$) | $Q_P$ | $Q_S$ |
|---|---|---|---|---|---|
| *Crust Model* 1 | | | | | |
| 30.0 | 6.30 | 3.65 | 2.90 | 2000.0 | 2000.0 |
| ∞ | 8.20 | 4.70 | 3.30 | 2000.0 | 2000.0 |
| *Crust Model* 2 | | | | | |
| 18.0 | 6.00 | 3.50 | 2.80 | 2000.0 | 2000.0 |
| 6.0 | 6.30 | 3.65 | 2.90 | 2000.0 | 2000.0 |
| 6.0 | 6.70 | 3.90 | 3.10 | 2000.0 | 2000.0 |
| ∞ | 8.20 | 4.70 | 3.30 | 2000.0 | 2000.0 |

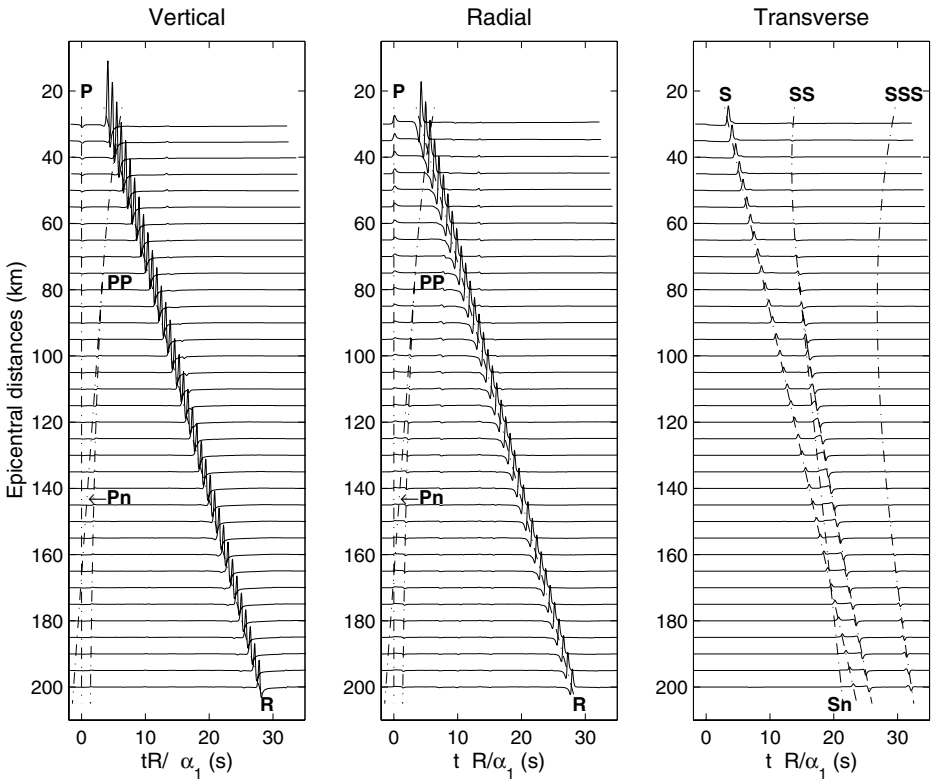


Figure 9

The synthetic three-component displacement seismograms for different epicentral distances, where reduced time $t - R/\alpha_1$ is used ($R$ is the epicentral distance, and $\alpha_1$ is the $P$ velocity in the top layer). Here, Crust Model 1 (see Table 3) is used, and the source and receivers are all at the free surface.

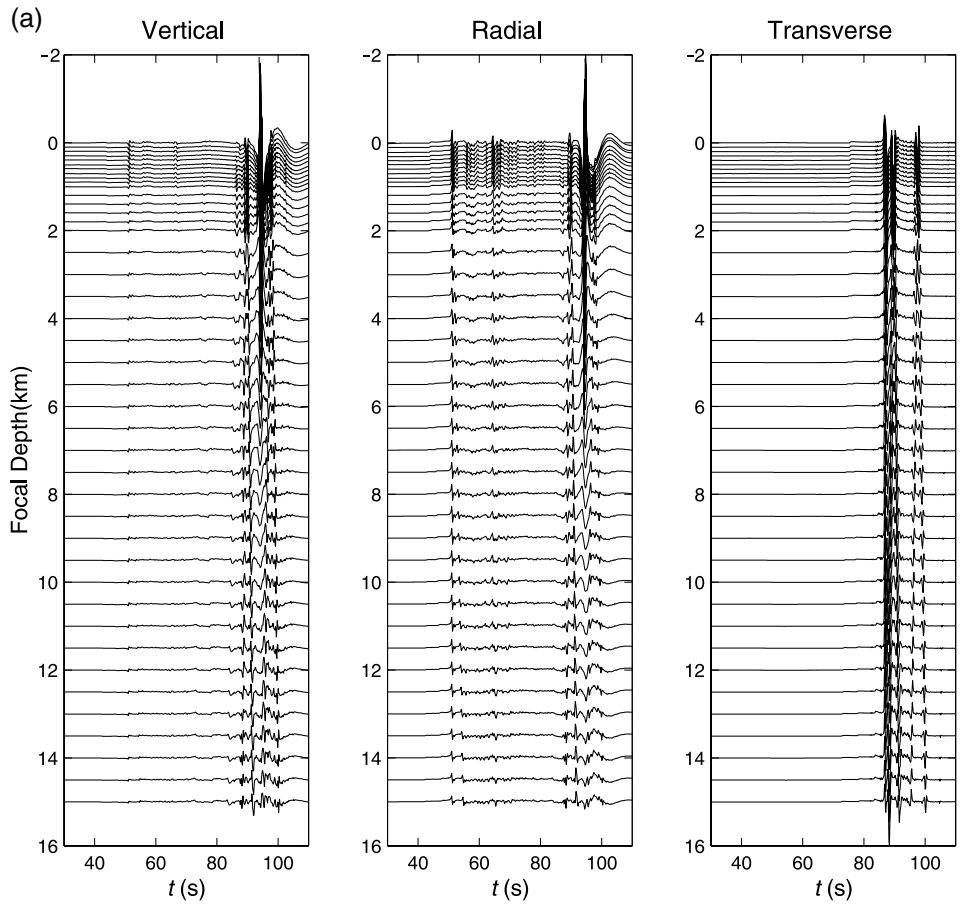


Figure 10
(a) The synthetic three-component displacement seismograms with different focal depths (0–15 km). Here, different focal depth steps are used for different depth ranges: 0.1 km for 0 to 1 km, 0.2 km for 1 to 2 km, and 0.5 km for 2 to 15 km. (b) and (c) The synthetic seismograms with a focal depth of 15 km obtained in this study and those in BOUCHON (1982), respectively. Crust Model 2 (see Table 3) is used, and the source a strike-slip double-couple point force. The receivers are at the surface with an epicentral distance of 300 km and an azimuth of 18°.

components are somewhat like the Lamb pulses, and we can see strong Rayleigh waves in both components, whereas for the transverse component, S, SS and SSS can be identified clearly.

We next consider a more complicated four-layer crust model (Crust Model 2, see Table 3). Here the source is also a strike-slip point double couple, and placed away from the free surface at a depth of 15 km. Different focal depth steps are used for different depth ranges: 0.1 km for 0 to 1 km, 0.2 km for 1 to 2 km, and 0.5 km for 2 to 15 km. The receiver is at the free surface with an epicentral distance of 300 km and

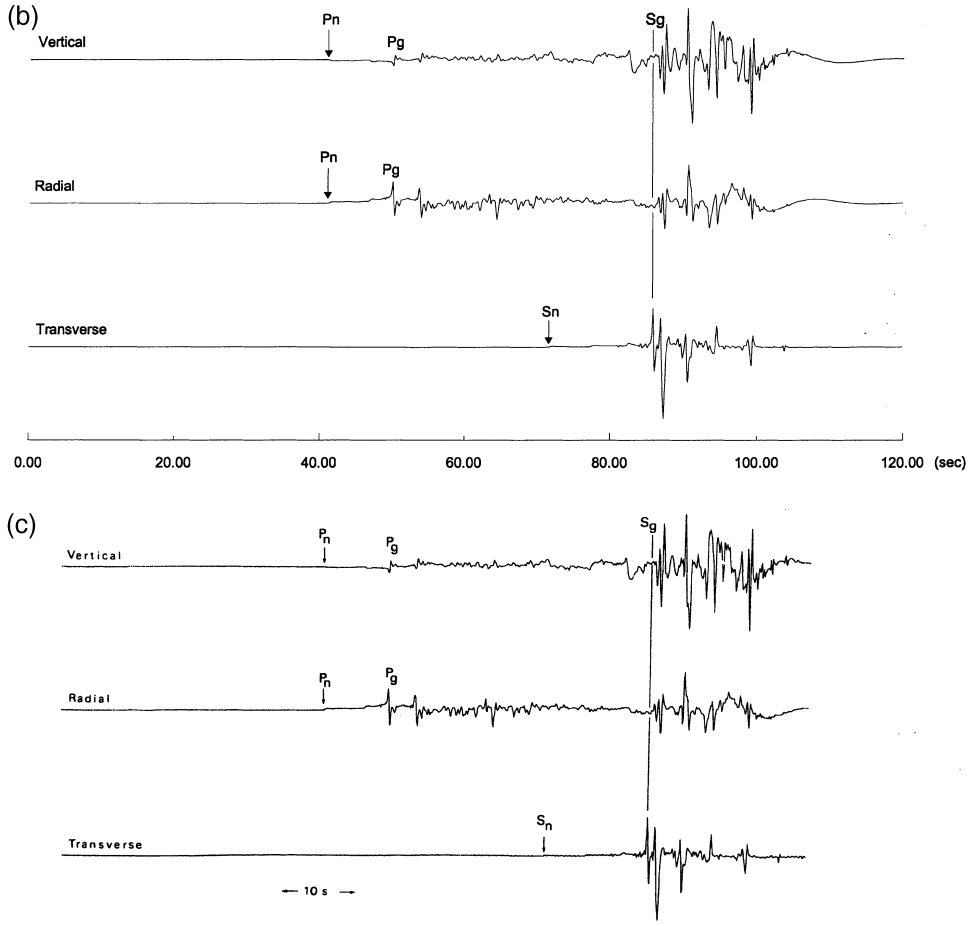


Figure 10b,c

an azimuth of 18°. The source time function matches the previous one. The result at a focal depth of 15.0 km obtained in this study and that in BOUCHON (1982) are shown in Figures 10(b) and (c), respectively. The excellent agreement between the two indicates that the result obtained by using our code is reliable. As shown in Figure 10(a), the synthetic displacement seismograms change continuously as focal depth decreases, which indicates that the results at shallow focal depths are reasonable.

## *Conclusions*

To efficiently calculate synthetic seismograms for a layered half-space with close to or the same depths, we proposed a simple while efficient method—the *Peak-*

*Trough Averaging Method* (PTAM), which is built upon the Repeated Averaging Method (DAHLQUIST and BJÖRCK, 1974; CHANG, 1988). Compared with the semi-analytic method (APSEL and LUCO, 1983; HISADA, 1994, 1995), this method is not only for simpler mathematically and easier to implement, but also more efficient. Using numerical examples, we illustrate that this method is accurate and efficient. Therefore, it is expected to be very useful in the computation of synthetic seismograms.

## *Acknowledgements*

The basic idea of this work was originally proposed by Dr. Shyhong Chang. Drs. Xiaofei Chen and Shyhong Chang would like to express their deepest gratitude to Prof. K. Aki for his guidance throughout the years of graduate study at USC. We thank Dr. B. Nowack and an anonymous reviewer for their critical comments and for the enhancement of English in the manuscript. This work is supported by the National Natural Sciences Foundation of China under grant of DYF49625406 and 40074008, and partially by the China National Fundamental Research Project (G1998040702).

## REFERENCES

AKI, K. and RICHARDS, P. Q., *Quantitative Seismology* (Freeman, San Francisco, 1980).

APSEL, R. J. and LUCO, J. E. (1983), *On the Green's Functions for a Layered Half-space. Part II*, Bull. Seismol. Soc. Am. *73*, 931–951.

BOUCHON, M. (1979), *Discrete Wavenumber Representation of Elastic Wave Fields in Three Space Dimensions*, J. Geophys. Res. *84*, 3604–3614.

BOUCHON, M. (1982), *The Complete Synthesis of Seismic Crustal Phases at Regional Distance*, J. Geophys. Res. *87*(B3), 1735–1741.

BOUCHON, M. and AKI, K. (1977), *Discrete Wavenumber Representation of Seismic Source Wave Fields*, Bull. Seismol. Soc. Am. *67*, 259–277.

CHANG, S. H. (1988), *Complete Wave-field Modeling and Seismic Inversion for Lossy-elastic Layered Half-space due to Surface Force*, Ph. D. Thesis, University of Southern California, Los Angeles.

CHEN, X. F. (1993), *A Systematic and Efficient Method of Computing Normal Modes for Multi-layered Half-space*, Geophys. J. Int. *115*, 391–409.

CHEN, X. F. (1999), *Seismograms Synthesis in Multi-layered Half-space Media. Part I. Theoretical Formulations*, Earthquake Res. in China *13*, 149–174.

DAHLQUIST, G. and BJÖRCK, Å., *Numerical Methods* (Prentice-Hall Inc., Englewood Cliffs, N. J., 1974).

DRAVINSKI, M. and MOSSESSIAN, T. K. (1988), *On Evaluation of the Green Function for Harmonic Line Loads in an Elastic Half-space*, J. Num. Meth. Engng. *26*, 823–841.

FUCHS, K. and MÜLLER, G. (1971), *Computation of Synthetic Seismograms with Reflectivity Method and Comparison with Observations*, Geophys. J. R. Astr. Soc. *23*, 417–433.

GRADSHTEYN, I. S. and RYZHIK, I. M., *Table of Integrals, Series, and Products* (Academic Press, New York, 1980).

HELMBERGER, D. V. (1974), *Generalized Ray Theory for Shear Dislocations*, Bull. Seismol. Soc. Am. *64*, 45–64.

HISADA, Y. (1994), *An Efficient Method for Computing Green's Functions for a Layered Half-space with Sources and Receivers at Close Depths*, Bull. Seismol. Soc. Am. *84*, 1457–1472.

HISADA, Y. (1995), *An Efficient Method for Computing Green's Functions for a Layered Half-space with Sources and Receivers at Close Depths (Part 2)*, Bull. Seismol. Soc. Am. *85*, 1080–1093.

KENNETT, B. L. N. *Seismic Wave Propagation in Stratified Media* (Cambridge University Press, New York, 1983).

KENNETT, B. L. N. and KERRY, N. J. (1979), *Seismic Waves in a Stratified Half space*, Geophys. J. R. Astr. Soc. *57*, 557–583.

LAMB, H. (1904), *On the Propagation of Tremors over the Surface of an Elastic Solid*, Phil. Trans. Roy. Soc. (London) A *203*, 1–42.

LUCO, J. E. and APSEL, R. J. (1983), *On the Green's Functions for a Layered Half-space. Part I*, Bull. Seismol. Soc. Am. *73*, 909–929.

RICKER, N. H., *Transient Waves in Visco-elastic Media* (Elsevier Scientific Publishing Co., Amsterdam, Holland, 1977).

WANG, C. Y. and HERRMANN, R. B. (1980), *A Numerical Study of P-, SV-, and SH-wave Generation in Plane-layered Medium*, Bull. Seismol. Soc. Am. *70*, 1015–1036.

YAO, Z. X. and HARKRIDER, D. G. (1983), *A Generalized Reflection-transmission Coefficient Matrix and Discrete Wavenumber Method for Synthetic Seismograms*, Bull. Seismol. Soc. Am. *73*, 1685–1699.

(Received December 11, 2000, accepted April 10, 2001)